Luteolin-Loaded Hyaluronidase Nanoparticles with Deep Tissue Penetration Capability for Idiopathic Pulmonary Fibrosis Treatment

Bo Pan[#], Fangping Wu[#], Shanming Lu, Wenwen Lu, Jiahui Cao, Fei Cheng, Mei tong Ou, Youyi Chen, Fan Zhang, Guolin Wu*, Lin Mei**

B. Pan, F. P. Wu, W. W. Lu, F. Cheng, Y. Y. Chen, G. L. Wu

The First Affiliated Hospital, Zhejiang University School of Medicine, 79 Qingchun Road, Hangzhou 310003, China

E-mail: wuguolin28@zju.edu.cn (G.L. Wu)

J. H. Cao, M. T. Ou, F. Zhang, L. Mei

State Key Laboratory of Advanced Medical Materials and Devices, Tianjin Key Laboratory of Biomedical Materials, Key Laboratory of Biomaterials and Nanotechnology for Cancer Immunotherapy, Institute of Biomedical Engineering, Chinese Academy of Medical Sciences and Peking Union Medical College, Tianjin 300192, China

E-mail: zhangfan@bme.pumc.edu.cn (F. Zhang), meilin@bme.pumc.edu.cn (L. Mei)

S. M. Lu, F. Zhang

Department of Pathology, Longgang Central Hospital, Shenzhen, Guangdong 518100, China

Idiopathic pulmonary fibrosis (IPF) is a chronic, progressive interstitial lung disease characterized by sustained fibrotic lesions. Orally administered drugs usual fail to efficiently penetrate the interstitial tissue and reach the lesions, resulting in low treatment efficiency. Luteolin is a natural flavonoid, active metabolites of which possess antioxidant, anti-inflammatory, anti-fibrotic, and anti-apoptotic properties. In this study, a nano-formulation was developed by loading luteolin into hyaluronidase nanoparticles (Lut@HAase). These Lut@HAase nanoparticles (NPs) exhibit small size and good stability, suitable for noninvasive inhalation and accumulation in the lungs, and hyaluronidase at the site of lesions can degrade hyaluronic acid in the interstitial tissue, enabling efficient penetration of luteolin. Luteolin's therapeutic effect, when administered via NPs, was studied both in vitro (using MRC5 cells) and in vivo (using IPF mice models), and its anti-fibrotic properties were found to inhibit inflammation and eliminate reactive oxygen species. Conclusively, this study demonstrates that Lut@HAase can improve lung function and enhance survival rates while reducing lung damage with few abnormalities during IPF treatment.

1. Introduction

Idiopathic pulmonary fibrosis (IPF) is a chronic and progressive interstitial lung disease that results in gas-exchange dysfunction and respiratory failure.[1] IPF affects approximately five million individuals worldwide.[2] The principal pathological manifestations of IPF are a consequence of repetitive injury to the alveolar epithelium, which drives dysregulated repair processes and leads to the recruitment of downstream effector cells and secretion of multiple cytokines and fibrotic factors.[3] The secreted profibrogenic factors initiate epithelial-to-mesenchymal transition (EMT) and fibroblast-to-myofibroblast transdifferentiation (FMT). Myofibroblasts are apoptosis-evading cells primarily responsible for the deposition and organization of the extracellular matrix and contribute to the formation of abnormal hypertrophic scarring or fibrosis.[4] These pathological changes destroy the structure of the alveoli and affect pulmonary ventilation.

Currently, pirfenidone and nintedanib are approved for IPF treatment owing to their anti-inflammatory and anti-fibrosis effects achieved via downregulation a variety of cytokines.[5] However, the failure of pirfenidone and nintedanib to halt or reverse disease progression, and their unclear mechanisms of action make them sub-optimal treatments.[6] Moreover, oral drug deliveries to the fibrotic lesions through blood circulation hinder drug accumulation.[7] Therefore, the identification of safe and effective drug therapies has emerged as a prominent focus in IPF research.[8]

Luteolin (3’,4’,5,7-tetrahydroxyflavone, Lut) is a natural flavonoid. It is mainly found in medicinal plants such as *Honeysuckle*, *Chrysanthemum*, *Schizogenetic*, *Prunella vulgaris*, *Perilla*, and *Scutellaria*, and has anti-inflammatory properties that can aid in relieving phlegm, cough, and asthma symptoms.[9] Active metabolites or derivatives of Lut have been reported to possess antioxidant, anti-inflammatory, anti-fibrosis, anti-apoptotic, anti-allergic, and anti-tumor properties.[10] Lut has been found to alleviate bronchoconstriction and airway hyperreactivity in ovalbumin-sensitized mice.[11] Additionally, it could decrease the acute *Chlamydia pneumoniae* infection load and inflammatory reactions in the lung tissue of infected mice.[12] Lut has also been shown to alleviate lung inflammation and fibrosis in bleomycin (BLM)-instilled C57BL/6 mice and inhibit the TGF-β1-stimulated myofibroblast differentiation and EMT *in vitro*.[13] However, direct use of Lut in IPF can’t be fully used due to its short half-life in the body. Moreover, the infiltration effect of Lut into the lesion site is very likely to be interfered by the physiological barrier of dense lung.

Chronic and sustained injuries to the alveoli characterizing IPF are accompanied by increased levels of hyaluronic acid (HA), which plays a role in depositing of extracellular matrix (ECM)

as well as regulating tissue injury and repair.[14] HA, following interaction with proteoglycans, such as aggrecan and versican, participates in the organization of fibrin, fibronectin (FN), and collagen.[15] The course of BLM-induced fibrosis is characterized by a significant increase in the concentration of HA in the lung parenchyma in animals.[16] The degradation of HA via, for example, hyaluronidase, which could digest the ECM and thus delay the progression of IPF.[17] The current IPF treatment can be significantly improved by increasing drug accumulation and efficacy. Here, we developed a nano-formulation of Lut loaded hyaluronidase NPs (denoted as Lut@HAase),[18] which could locally accumulate in the lungs to treat IPF via noninvasive inhalation (**Scheme 1**). The inhaled Lut@HAase could deposit in the alveoli, subsequently penetrate the interstitial fibrotic foci. We confirmed that the released hyaluronidase from Lut@HAase could degrade HA in the interstitial tissue, facilitating Lut penetration into the lesion more efficiently. Furthermore, Lut@HAase inhibits inflammatory cytokines secrete, and promotes the scavenging of oxygen free radicals (ROS). Thus, Lut@HAase can accelerate the clearance of excess collagen, inhibit fibrosis, synergistically restore alveolar integrity, and improve lung function.

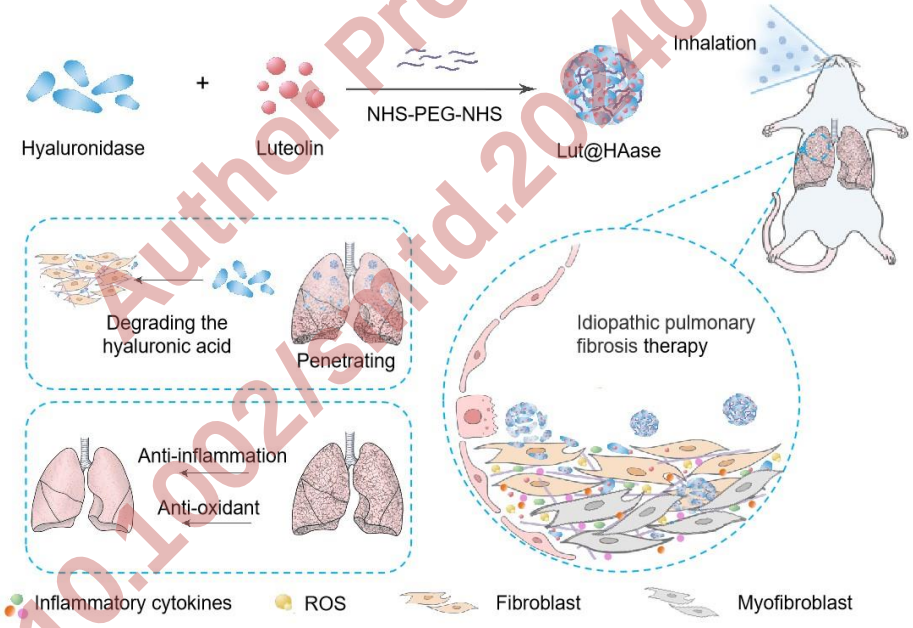

Scheme 1. Schematic illustration of Lut@HAase with efficient antifibrotic performance for treatment of IPF.

2. Results and discussion

2.1 Construction and characterization of Lut@HAase

Lut@HAase were synthesized via one-pot approach using NHS-PEG1000-NHS as cross-linkers **(Figure 1**a**)**. Lut@HAase exhibited a spherical morphology with good monodispersity, as observed using transmission electron microscope (TEM) (Figure 1b). The hydrodynamic

diameter of Lut@HAase was approximately 100 nm (Figure 1c). Lut was successfully loaded in Lut@HAase (loading rate, 9.3%) as detected using high-performance liquid chromatography (HPLC) (Figure S1, Supporting Information). Considering the antioxidant potential of Lut, ROS-scavenging by Lut@HAase was detected using electron spin resonance (ESR) spectroscopy. As shown in Figure 1d, Lut@HAase, as well as free Lut, was able to scavenge superoxide anions (O_2•−) and hydroxyl radicals (•OH), confirming the antioxidant profile of Lut@HAase. In addition, there was almost no change in the particle size or polymer dispersity index after one week of storage in phosphate-buffered saline (PBS) (Figure 1e), indicating good stability of Lut@HAase. We further tested the stability of Lut@HAase before and after lyophilization (Figure 1f). No variation was observed in the stability of NPs before and after lyophilization. The release of luteolin from Lut@HAase at different points of time and the cytotoxicity of NPs were also measured as shown in Figure S2, Figure S3 and Figure S4, supporting information.

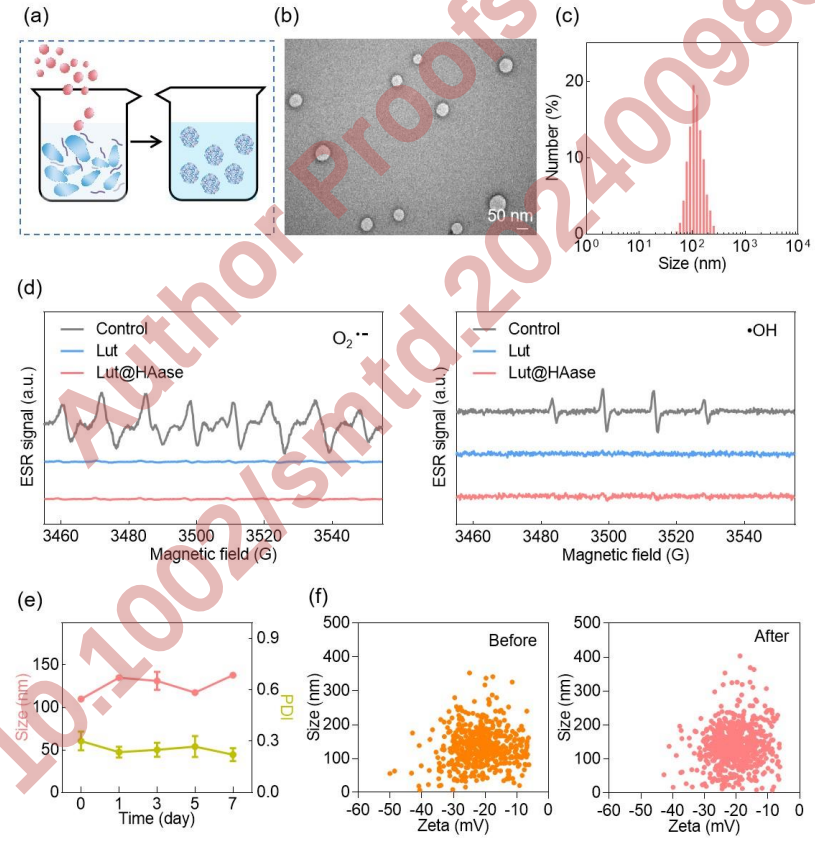

Figure 1. Construction and characterization of Lut@HAase. (a) Schematic illustration of Lut@HAase preparation. (b) TEM image of Lut@HAase. (c) Size of Lut@HAase. (d) ESR spectra of O_2•− and •OH after treatment with free Lut or Lut@HAase. (e) Stability of Lut@HAase over one week of storage in PBS. (f) Stability of Lut@HAase before and after lyophilization.

2.2 Lut@HAase suppress TGF-β1-induced fibrosis in MRC5 cells

To examine whether Lut@HAase could reduce the degree of fibrosis, human embryonic lung fibroblast MRC5 cells were used to simulate pulmonary fibrosis (Figure S5, Supporting Information). Stimulation of resting lung fibroblasts with TGF-β1 promoted the expression of α-smooth muscle actin (α-SMA), indicating myofibroblasts. In addition to Lut@HAase, hyaluronidase NPs (denoted as HAase) of comparable sizes were also synthesized in this study. As shown in **Figure 2**a, compared with PBS group, HAase group did not show significant suppression of α-SMA expression in MRC5 cells promoted with TGF-β1. Lut could inhibit α-SMA expression, which is consistent with literature report.[19] Compared with Lut group, treatment with Lut@HAase more significantly repressed the expression levels of α-SMA. This result suggests that HAase can assist Lut suppress the profibrotic progress of MRC5 cells induced by TGF-β1 stimulatory effects. A possible explanation is that loading Lut into HAase promoted more efficient entry of Lut into cells to exert its anti-fibrosis effects. This finding is consistent with the flow cytometry analysis which also confirmed that Lut@HAase inhibited TGF-β1-induced α-SMA expression (Figure S6, Supporting Information).

The suppression of the profibrotic effect of Lut@HAase was further verified via immunofluorescence staining and flow cytometry analysis of FN expression, which is a marker protein for IPF (Figure 2b, Figure S7, Supporting Information). Compared to the results from the PBS group, the treatment with Lut@HAase significantly suppressed FN expression, by nearly six-folds.

Furthermore, the inflammatory cytokines of MRC5 cells were measured after exposure to TGF-β1. As shown in Figure 2c (Table. S1, Supporting Information), the levels of IL-6, IL-1β, and TNF-α increased noticeably after TGF-β1 stimulation. Compared with the PBS or HAase treatment groups, the Lut group exhibited a decrease in cytokine secretion. This effect was ameliorated when Lut and hyaluronidase were integrated into Lut@HAase. The loading of Lut into NPs facilitates the stability and endocytosis of Lut by cells and exert its function, further suppressing the secretion of IL-6, IL-1β, and TNF-α. Therefore, Lut@HAase effectively reduced the release of these inflammatory cytokines compared to the other groups, thereby showing better anti-inflammatory effects.

It is also worth mentioning that the potential ROS clearance by Lut in fibrotic cells could, in turn, help to arrest the progression of fibrosis. To assess the effectiveness of Lut@HAase in ROS clearance, the cellular levels of ROS in MRC5 cells after the indicated treatment were measured using flow cytometry. Figure 2d clearly shows that the cellular ROS levels

increased after TGF-β1 stimulated. Following treatment with Lut or Lut@HAase, the mean fluorescence intensity (MFI) of intracellular ROS in MRC5 cells decreased (Figure 2e). Notably, the Lut@HAase group exhibited more effective ROS clearance than the Lut group. These findings suggest that the combination of hyaluronidase and Lut synergistically enhances ROS clearance.

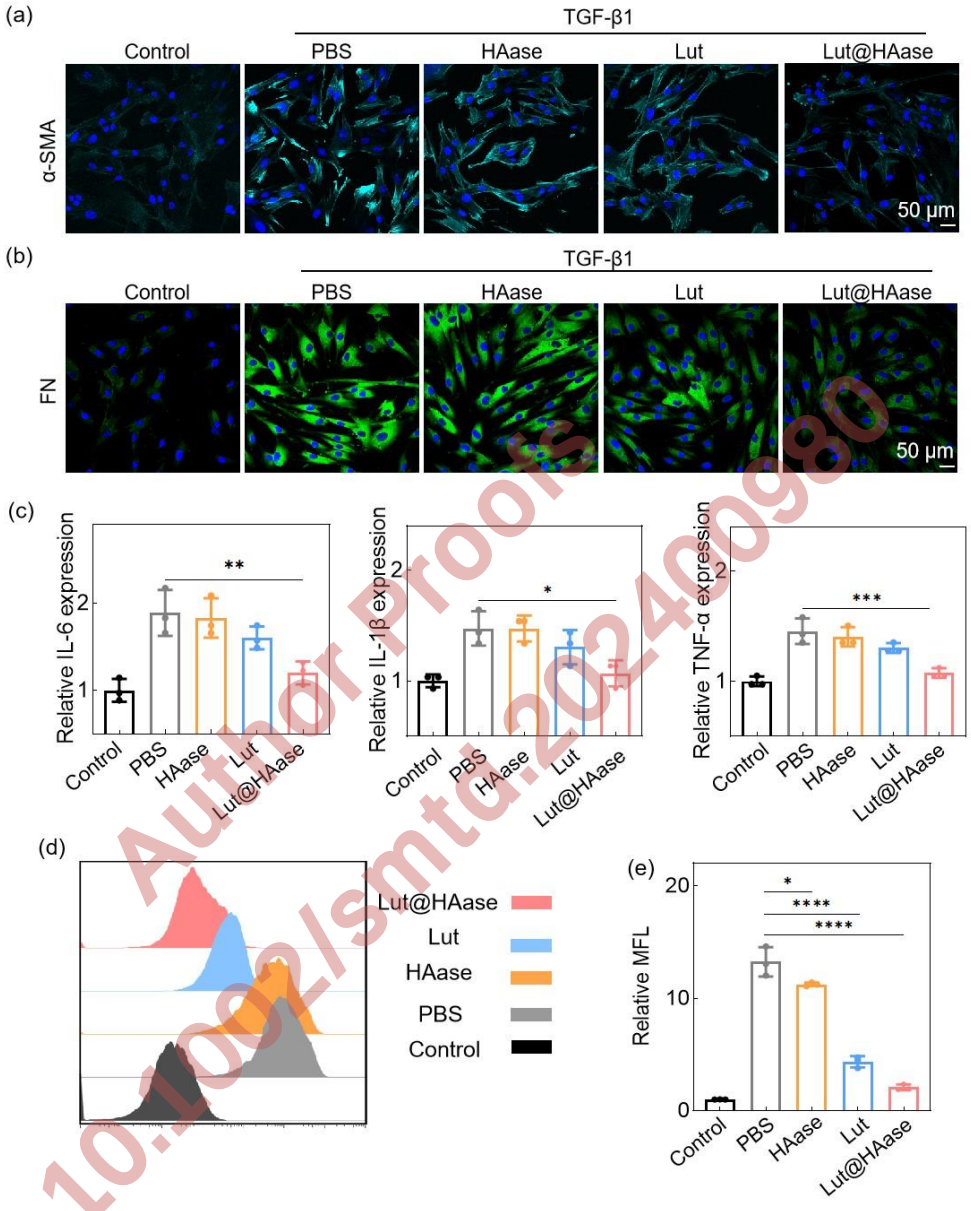

Figure 2. Evaluations the anti-fibrotic, anti-inflammatory, and antioxidant effect of Lut@HAase *in vitro*. (a), (b) Representative fluorescence images of α-SMA or FN expression of MRC5 cells after the indicated treatments (blue: nuclei; green: α-SMA/FN; scale bars: 50μm). (c) The levels of IL-6, IL-1β, and TNF-α in the supernatant of MRC5 cells after the indicated treatments (n = 3). The flow cytometry histogram (d) and quantitative analysis (e) for potential ROS clearance of different treatments for fibrotic cells (n = 3). Quantitative data

in (c) and (e) are presented as mean ± SD. Statistical significance was assessed using one-way analysis of variance (ANOVA). *p < 0.05, **p < 0.01, ***p < 0.005, ****p < 0.001.

2.3 Accumulation of Lut@HAase in the lung tissue and penetration ability

Since the lung accumulation performance of Lut@HAase was highly correlated with the subsequent anti-fibrosis effect, we next focused our attention on the biodistribution behavior of these NPs. Intravenous (*i.v.*) injection and inhalation were the two routes of administration tested to determine the optimal route for efficient accumulation of Lut@HAase in a mouse model of BLM-induced fibrosis. The time-elapsed fluorescent signals of Lut@HAase (labeled with DiR dye) were compared. As shown in **Figure 3**a, Lut@HAase fluorescence signals were observed at the lung site 1 h after *i.v.* injection or inhalation, indicating that Lut@HAase can accumulate in the lung. At 9 h post-administration, Lut@HAase accumulation was highest in the lungs after inhalation. The peak value in the inhalation group was nearly three times higher than *i.v.* injection group (Figure 3b). The distribution of Lut@HAase in major organs was further evaluated. As shown in Figure 3c and 3d, in the inhalation group, Lut@HAase were primarily accumulated in the lungs. In contrast, in the *i.v.* injection group, Lut@HAase showed large accumulation in the liver, with almost no signal was detected in the lungs at day 5 post-injection. This phenomenon was further confirmed by immunofluorescence sectioning (Figure 3e and Figure S8, Supporting Information). These results indicated that Lut@HAase administration via inhalation resulted in better lung accumulation than that with *i.v.* injection.

Having demonstrated the accumulation at lung site of Lut@HAase, we further evaluated the penetration into lung tissue. We established an *in vitro* model of the interstitial environment of lung fibrocytes by cultivating MRC5 cell spheres. As shown in Figure 3f, we observed the Lut@HAase (indicated by red fluorescent signals) disperse throughout the cell spheres (III), showing good penetration ability of Lut@HAase with the help of hyaluronidase degrading HA. However, once the Lut@HAase were pre-crosslinked with glutaraldehyde, numbers of Lut@HAase were restricted around the cell spheres, showing inefficient penetration caused by the obstruction of the dense intercellular substance (II). These reflected the importance of loading Lut into HAase NPs for favorable deep delivery performance.

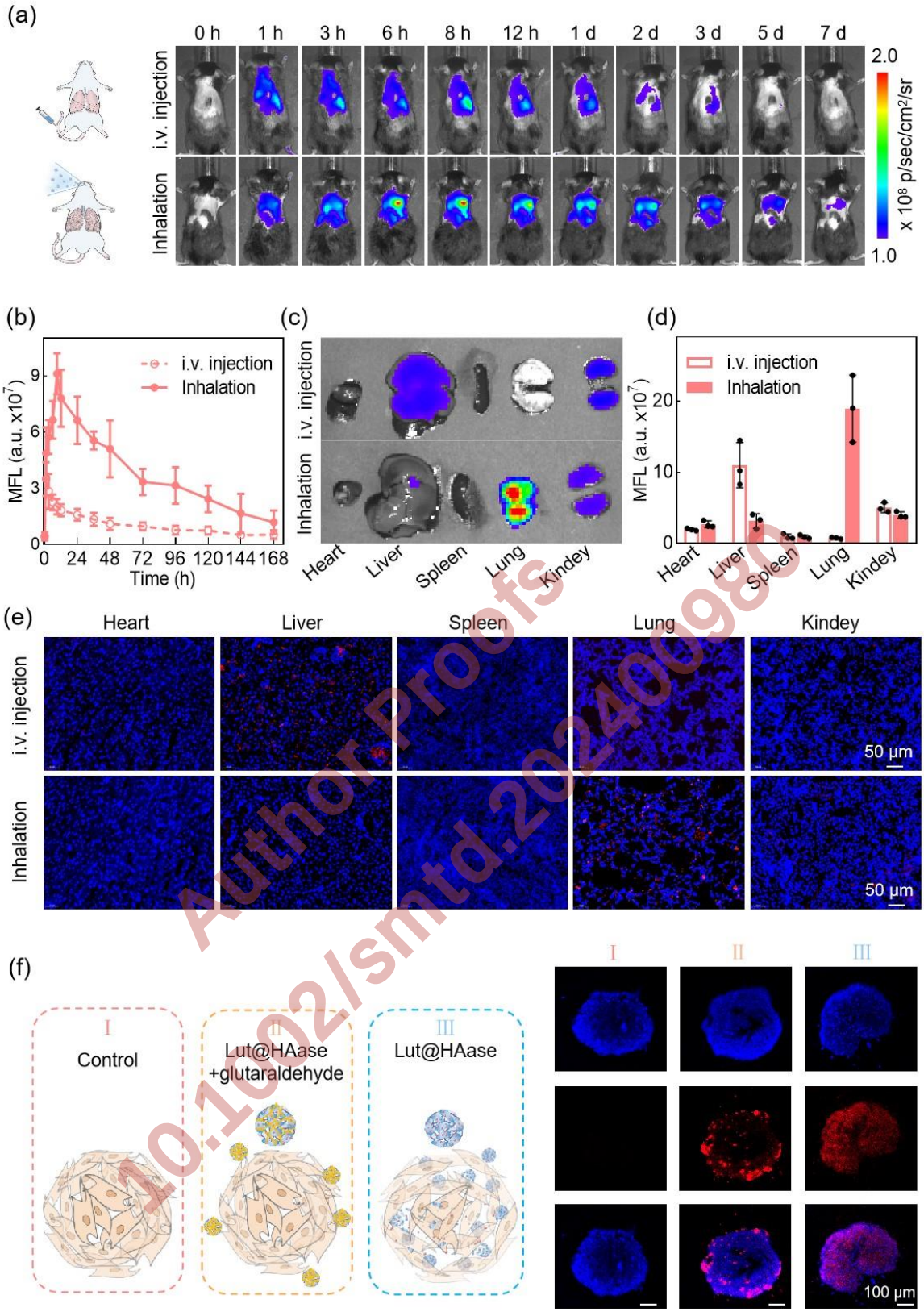

Figure 3. Distribution and penetration of Lut@HAase. (a) *In vivo* real-time Lut@HAase. (b) The MFI of Lut@HAase in lung with *i.v.* injection or inhalation. (c) *Ex-vivo* fluorescence imaging of major organs of mice at day 5 after different administrations. (d) The MFI of Lut@HAase in major organs with *i.v.* injection or inhalation. (e) Confocal laser scanning

microscopy (CLSM) imaging of major organs tissues infiltrated with Lut@HAase at day 5 after *i.v.* injection or inhalation. (red: Lut@HAase; blue: nucleus; scale bar: 50μm). (f) Schematic illustration of the penetration process of Lut@HAase; CLSM images of Lut@HAase penetration in the MRC5 cell spheres. Lut@HAase with the addition of glutaraldehyde is referred to as Lut@HAase + glutaraldehyde (blue: nucleus; red: Lut@HAase; scale bar: 100 μm)

2.4 Therapeutic effects of Lut@HAase

We further evaluated the therapeutic effects of Lut@HAase. The BLM-induced pulmonary fibrosis mice were randomly categorized into four groups that were treated with PBS, HAase, Lut, or Lut@HAase via inhalation using a nebulizer every 3 days from day 5 to 17 **(Figure. 4a)**. On day 22, various parameters were evaluated to assess therapeutic outcomes. Healthy mice served as controls. As shown in Figure 4b (Figure S9, Supporting Information) lung resistance (RL) was significantly elevated in mice with BLM-induced fibrosis, indicating a reduction in lung contraction and elasticity due to BLM-induced injury. Interestingly, treatment with Lut@HAase relieved this trend, leading to a marked improvement in the RL. Compared with the control group, the pulmonary function parameters of forced vital capacity (FVC), dynamic compliance (Cdyn), expiratory reserve volume (ERV), peak expiratory flow (PEF), and forced expiratory volume in the first 0.2 s (FEV0.2) were all observed to decrease following BLM-induced injury. Following treatment with Lut@HAase, these parameters increased, indicating that Lut@HAase caused recovery of lung function. The reversal of the lung function decline by Lut@HAase treatment highlights its potential therapeutic value in BLM-induced fibrosis.

Total protein content in the bronchoalveolar lavage fluid (BALF) was evaluated as an indicator of lung injury. The total protein content in BALF was elevated after BLM challenge (PBS group) but was decreased by Lut@HAase treatment (Figure 4c). Alongside with the improved lung function, Lut@HAase treatment also improved the life cycle and reduced the mortality rate (Figure 4d). Nine of ten mice treated with Lut@HAase survived through the 22 days, indicating a sharp improvement in overall survival compared with mice treated with PBS. These data strongly suggested the significant anti-fibrotic performance of Lut@HAase.

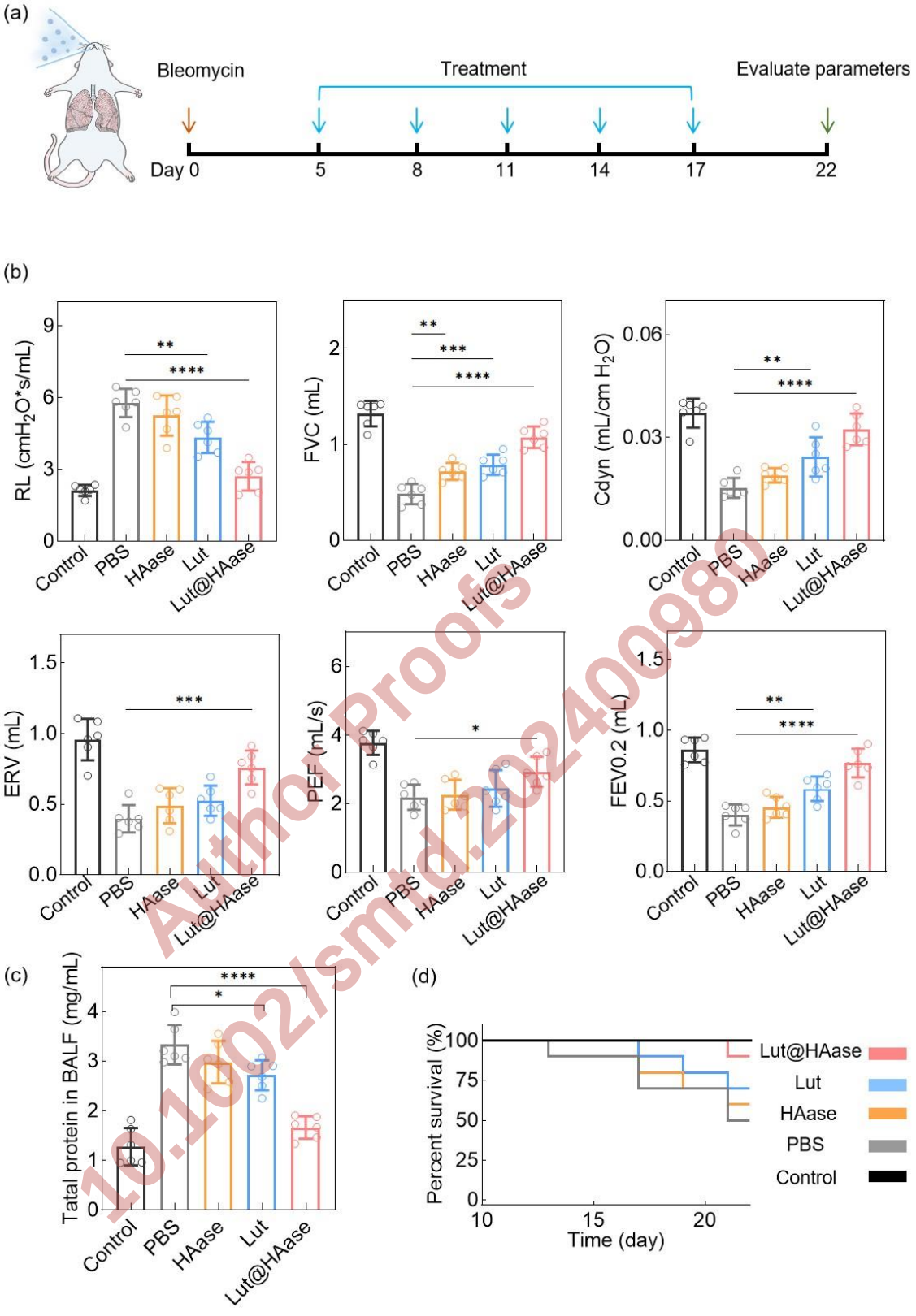

Figure 4. Therapeutic effects of Lut@HAase in a BLM-induced fibrosis mouse model. (a) Schematic illustration of therapeutic schedule. (b) The evaluation on pulmonary function of the model mice including RL, FVC, Cdyn, ERV, PEF, and FEV0.2 after different treatments (n = 6). (c) Determination of total protein content in BALF after different treatments (n = 6).

(d) Survival curve of BLM-induced fibrosis mice after different treatments. Quantitative data in (b) and (c) are presented as mean ± SD. Statistical significance was assessed using one-way analysis of variance (ANOVA). *p < 0.05, **p < 0.01, ***p < 0.005, ****p < 0.001.

2.5 The effect of Lut@HAase against idiopathic pulmonary fibrosis

We conducted another batch of experiments in which the lung tissues of the mice were collected. As shown in **Figure 5a**, compared to healthy (control) mice, BLM caused hemorrhagic necrosis in mouse lungs, a characteristic of pulmonary fibrosis, as revealed by initial histological examination. Lut@HAase showed curative effects against BLM-induced lung fibrosis, which was reflected by the marked reduction in damage in the Lut@HAase group.

Hematoxylin and eosin (H&E) staining of the lung tissue showed that, after Lut@HAase treatment, the lung interstitial cells returned to an elongated and flat morphology (Figure 5b). Similarly, Masson staining (Figure S10, Supporting Information) also showed the restorative effects on lung injury, as described above. Moreover, immunofluorescence staining of α-SMA was performed to assess the progress of myofibroblast activation and fibrosis (Figure 5c). The MFI results showed that α-SMA expression was reduced by Lut@HAase treatment, further confirming its antifibrotic effects (Figure 5d). Hydroxyproline content in the lung tissues was measured as a marker of collagen deposition, which is a key process in the development of pulmonary fibrosis. We further evaluated the level of lung hydroxyproline, which demonstrated that the hydroxyproline content was distinctly reduced in the Lut@HAase treated group compared with that in the HAase or Lut alone groups (Figure 5e).

We then to explore the anti-fibrosis mechanism of Lut@HAase by examining the levels of inflammatory factors and ROS in the lung tissue. The Lut@HAase noticeably lowers the levels of TGF-β1, IL-6, IL-1β, and TNF-α, which illustrates the cytokine reduction associated with tissue after fibrosis recovery (Figure 5f and 5g). Furthermore, compared with BLM-induced mice exposed to HAase or Lut alone, mice treated with Lut@HAase exhibited the closest ROS content to the control group (Figure 5h). These results suggested that Lut@HAase could act as anti-fibrosis agents via inhibited inflammatory cytokines secrete and mitigated oxidative stress.

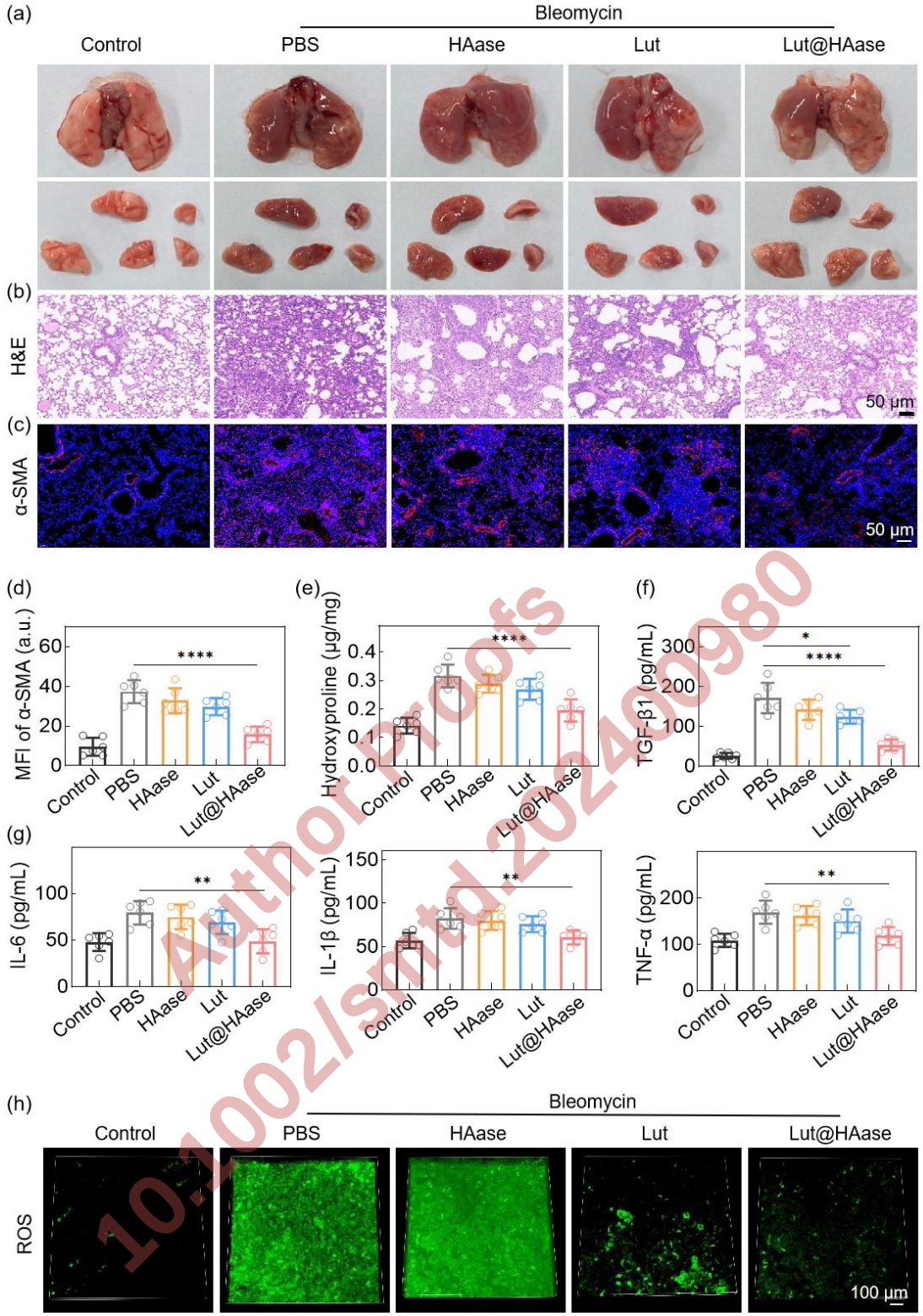

Figure 5. The anti-fibrosis effects and mechanism of Lut@HAase. (a) Representative images of lungs from mice treated with PBS, HAase, Lut or Lut@HAase after BLM challenge. H&E staining (b) and immunofluorescence staining of α-SMA (c) in lung section (Blue: nuclei; red: α-SMA; scale bars: 50μm). (d) Corresponding quantitative analysis of α-SMA MFI in (c). (e) Measurement of hydroxyproline content in mouse lung tissues (n = 6). (f) Quantification of

TGF-β1 level in BALF by ELISA (n = 6). (g) The levels of IL-6, IL-1β, and TNF-α in lung tissues (n = 6). (h) The levels of ROS in lung tissues from different treatment groups (green: ROS; scale bar: 100μm). Quantitative data in (d) to (g) are presented as mean ± SD. Statistical significance was assessed using one-way analysis of variance (ANOVA). *p < 0.05, **p < 0.01, ****p < 0.001.

2.6 The safety estimation of Lut@HAase

H&E staining results showed that there was no obvious damage to major organs in each group at the end of the experiment. Additionally, no obvious abnormality was found in urea nitrogen (BUN), lactate dehydrogenase (LDH), alanine amino transferase (ALT), aspartate transaminase (AST) and alkaline phosphatase (ALP) after different treatments (Figure S11 in Supporting information).

3. Conclusion

In this study, we constructed a Lut@HAase nano-formulation using hyaluronidase loaded with Lut and cross-linked with NHS-PEG-NHS.[20] Such a design incorporating recent nanoparticle technologies bestowed NPs with enhanced penetration features for the high-performance delivery of Lut in deep pulmonary fibrosis.[21] The synthesized Lut@HAase, with favorable properties of good size and stability, paved the way for noninvasive inhalation and local accumulation in the lungs to treat IPF. After administration via inhalation to a mouse model of pulmonary fibrosis, the hyaluronidase in Lut@HAase degraded HA in the interstitial tissue, allowing Lut-load NPs to penetrate the lesion more efficiently.[22] Consequently, Lut inhibited the inflammatory cytokines secrete, and also eliminated ROS, further contributing to its antifibrotic properties.[23] Conclusively, these Lut@HAase can alleviate respiratory dysfunction, improve lung contraction and elasticity, and enhance survival rates, while reducing lung damage with few abnormalities. These satisfactory results generated by the synergistic strategy suggest that our engineered Lut@HAase could serve as a promising modality for safe and high-performance IPF therapy.

Supporting Information

Supporting Information is available from the Wiley Online Library or from the author

Acknowledgements

The animal experimental protocols were reviewed and approved by the Zhejiang University First Affiliated Hospital, with approval number 1147. B. Pan and F. P. Wu contributed equally to this work. The authors gratefully acknowledge the support of this research by

Natural Science Foundation of Zhejiang Province Public Welfare Project (LTGY23H100002); Natural Science Foundation of Zhejiang Province Exploration Project (LQ21H160021); Natural Science Foundation of Zhejiang Province Public Welfare Project (LTGY24H270001); Natural Science Foundation of Tianjin (23JCYBJC00470); Ningbo Natural Science Foundation of China (2021J016); The Key Project Jointly built by the State Administration of Traditional Chinese Medicine and Zhejiang Provincial Administration of Traditional Chinese Medicine (GZY-ZJ-KJ-23075) and Medical health technology innovation project of Chinese Academy of Medical Sciences (2021-I2M-1-058).

Conflict of Interest

The authors declare no conflict of interest.

Data Availability Statement

The data that support the findings of this study are available from the corresponding author upon reasonable request.

Keywords

idiopathic pulmonary fibrosis, nanoparticles, luteolin, hyaluronidase, penetration, anti-fibrosis

Received: ((will be filled in by the editorial staff))

Revised: ((will be filled in by the editorial staff))

Published online: ((will be filled in by the editorial staff))

References

[1] a) A. J. Podolanczuk, C. C. Thomson, M. Remy-Jardin, L. Richeldi, F. J. Martinez, M. Kolb, G. Raghu, *Eur. Respir. J.* **2023**, *61*; b) S. Gandhi, R. Tonelli, M. Murray, A. V. Samarelli, P. Spagnolo, *Int. J. Mol. Sci.* **2023**, *24*; c) P. Spagnolo, J. A. Kropski, M. G. Jones, J. S. Lee, G. Rossi, T. Karampitsakos, T. M. Maher, A. Tzouvelekis, C. J. Ryerson, *Pharmacol. Ther.* **2021**, *222*, 107798.

[2] E. Farrand, C. Iribarren, E. Vittinghoff, T. Levine-Hall, B. Ley, G. Minowada, H. R. Collard, *Chest* **2021**, *159*, 219.

[3] a) B. J. Moss, S. W. Ryter, I. O. Rosas, *Annu. Rev. Pathol.* **2022**, *17*, 515; b) S. J. Dorry, B. O. Ansbro, D. M. Ornitz, G. M. Mutlu, R. D. Guzy, *Am. J. Respir. Cell. Mol. Biol.* **2020**, *62*, 608.

[4] a) F. Luppi, M. Kalluri, P. Faverio, M. Kreuter, G. Ferrara, *Respir. Res.* **2021**, *22*, 109; b) K. Isobe, T. Issiki, S. Sakamoto, G. Sano, Y. Takai, N. Tochigi, S. Homma, *J. Thorac. Dis.* **2019**, *11*, 2981.

[5] a) S. Wang, W. Rao, A. Hoffman, J. Lin, J. Li, T. Lin, A. A. Liew, M. Vincent, T. Mertens, H. Karmouty-Quintana, C. P. Crum, M. L. Metersky, D. A. Schwartz, P. Davies, C. Stephan, S. Jyothula, A. Sheshadri, E. E. Suarez, H. J. Huang, J. F. Engelhardt, B. F.

Dickey, K. R. Parekh, F. D. Mckeon, W. Xian, *Sci. Transl. Med.* **2023**, *15*, eabp9528; b) F. Bonella, P. Spagnolo, C. Ryerson, *Drugs* **2023**, *83*, 1581.

[6] a) D. M. Kopustinskiene, V. Jakstas, A. Savickas, J. Bernatoniene, *Nutrients* **2020**, *12*; b) G. Raghu, W. C. Johnson, D. Lockhart, Y. Mageto, *Am. J. Respir. Crit. Care Med.* **1999**, *159*, 1061.

[7] a) L. Huang, M. Y. Kim, J. Y. Cho, *Int. J. Mol. Sci.* **2023**, *24*; b) Z. Calis, R. Mogulkoc, A. K. Baltaci, *Mini-Rev. Med. Chem.* **2020**, *20*, 1475; c) N. Aziz, M. Y. Kim, J. Y. Cho, *J. Ethnopharmacol.* **2018**, *225*, 342.

[8] a) J. A. Peruzzi, T. Q. Vu, T. F. Gunnels, N. P. Kamat, *Small Methods* **2023**, *7*, e2201718; b) J. Chen, J. Tan, J. Li, W. Cheng, L. Ke, A. Wang, Q. Wang, S. Lin, G. Li, B. Wang, J. Chen, P. Zhang, *Small Methods* **2023**, *7*, e2300678; c) T. Yudhistira, S. E. Da, A. Combes, M. Lehmann, A. Reisch, A. S. Klymchenko, *Small Methods* **2023**, *7*, e2201452.

[9] a) H. Xu, W. Yu, S. Sun, C. Li, Y. Zhang, J. Ren, *Front. Physiol.* **2020**, *11*, 113; b) W. B. Zhou, Z. N. Miao, B. Zhang, W. Long, F. X. Zheng, J. Kong, B. Yu, *Neural Regen. Res.* **2019**, *14*, 613.

[10] a) Y. Q. He, C. C. Zhou, L. Y. Yu, L. Wang, J. L. Deng, Y. L. Tao, F. Zhang, W. S. Chen, *Pharmacol. Res.* **2021**, *163*, 105224; b)K. Iida, T. Naiki, A. Naiki-Ito, S. Suzuki, H. Kato, S. Nozaki, T. Nagai, T. Etani, Y. Nagayasu, R. Ando, N. Kawai, T. Yasui, S. Takahashi, *Cancer Sci.* **2020**, *111*, 1165; c) E. Papakonstantinou, I. Bonovolias, M. Roth, M. Tamm, D. Schumann, F. Baty, R. Louis, B. Milenkovic, W. Boersma, B. Stieltjes, K. Kostikas, F. Blasi, J. G. Aerts, G. Rohde, A. Lacoma, A. Torres, T. Welte, D. Stolz, *Eur. Respir. J.* **2019**, *53*.

[11] M. Shi, Z. Chen, H. Gong, Z. Peng, Q. Sun, K. Luo, B. Wu, C. Wen, W. Lin, *Phytother. Res.* **2024**, *38*, 880.

[12] S. Gao, Y. Gao, L. Cai, R. Qin, *Microbiol. Spectr.* **2024**, *12*, e327923.

[13] X. Ren, T. Yang, K. Zhang, Y. Liu, C. Wang, L. Wu, J. Zhang, *Int. J. Pharm.* **2023**, *645*, 123405.

[14] a) K. Mandal, A. D. Raz-Ben, Z. T. Graber, B. Wu, C. Y. Park, J. J. Fredberg, W. Guo, T. Baumgart, P. A. Janmey, *ACS Nano* **2019**, *13*, 203; b) F. Rivas, O. K. Zahid, H. L. Reesink, B. T. Peal, A. J. Nixon, P. L. Deangelis, A. Skardal, E. Rahbar, A. R. Hall, *Nat. Commun.* **2018**, *9*, 1037.

[15] a) Y. Xin, P. Xu, X. Wang, Y. Chen, Z. Zhang, Y. Zhang, *Stem Cell Res. Ther.* **2021**, *12*, 49; b) A. Lierova, J. Kasparova, J. Pejchal, K. Kubelkova, M. Jelicova, J. Palarcik, L. Korecka, Z. Bilkova, Z. Sinkorova, *Front. Pharmacol.* **2020**, *11*, 1199; c) A. Betensley, R. Sharif, D. Karamichos, *J. Clin. Med.* **2016**, *6*.

[16] S. Wang, S. H. Yu, *Small Methods* **2024**, *8*, e2301487.

[17] a) Y. Qu, B. Chu, J. Li, H. Deng, T. Niu, Z. Qian, *Small Methods* **2023**, e2301178; b)S. N. Iyer, G. Gurujeyalakshmi, S. N. Giri, *J. Pharmacol. Exp. Ther.* **1999**, *289*, 211.

[18] a) Y. Ren, Z. Zhang, Y. She, Y. He, D. Li, Y. Shi, C. He, Y. Yang, W. Zhang, C. Chen, *Small Methods* **2024**, *8*, e2300747; b) S. Li, S. Jiang, M. Rahman, J. Mei, X. Wang, J. Jiang, Y. Chen, S. Xu, Y. Liu, *Small Methods* **2023**, *7*, e2201569.

[19] C. Y. Chen, W. H. Peng, L. C. Wu, C. C. Wu, S. L. Hsu, *J. Agric. Food. Chem.* **2010**, *58*, 11653.

[20] a) R. J. Connor, R. Clift, D. W. Kang, *Drug Deliv.* **2023**, *30*, 2252999. b) M. Li, Y. Zhang, Q. Zhang, J. Li, *Mater. Today Bio* **2022**, *16*, 100364.

[21] H. Zhou, Z. Fan, J. Deng, P. K. Lemons, D. C. Arhontoulis, W. B. Bowne, H. Cheng, *Nano Lett.* **2016**, *16*, 3268.

[22] X. Hou, D. Zhong, Y. Li, H. Mao, J. Yang, H. Zhang, K. Luo, Q. Gong, Z. Gu, *J. Nanobiotechnology* **2021**, *19*, 111.

[23] K. Rakoczy, J. Kaczor, A. Soltyk, N. Szymanska, J. Stecko, J. Sleziak, J. Kulbacka, D. Baczynska, *Int. J. Mol. Sci.* **2023**, *24*.